Approximations to Channel Flows using Variational Principles

S. L. Wakelin

Numerical Analysis Report 10/92

Department of Mathematics
University of Reading
P. O. Box 220
Reading RG6 2AX

Abstract

Variational principles whose natural conditions are the steady state shallow water equations of motion are stated. The corresponding variational principles for quasi one-dimensional flows are derived. Discontinuous solutions of the shallow water equations are considered by formulating new variational principles, whose natural conditions include the relations between the flow variables immediately either side of a hydraulic jump.

Approximations to continuous and discontinuous flows in channels of varying breadths and constant equilibrium depths are calculated using finite dimensional versions of these variational principles. Approximations to continuous flows are calculated on fixed grids using both the quasi one-dimensional and the two-dimensional formulations. Methods of generating adaptive grids in one dimension using the variational principles are also studied and these allow grid dependent approximations to continuous and discontinuous quasi one-dimensional flows to be found.

1 Introduction

In a previous report [1] a number of variational principles for unsteady and steady continuous shallow water flows were derived. The continuous, differentiable functions which satisfy the variational principles also satisfy the shallow water equations of motion. Many principles are available because the governing physical laws can be expressed in different variables, and because each free principle can be used to formulate one or more constrained principles. The main purpose of this report is to use these variational principles to generate finite dimensional approximations to solutions of the shallow water equations for channel flows.

In [1] the variational principle devised by Luke [2] for fluid flow beneath a free surface was used as a starting point to form other principles for unsteady shallow water flows which were then modified for time-independent flows. In Section 2 of this report the shallow water equations of steady motion are stated and the corresponding variational principles for steady flows are given. By assuming that the flow is quasi one-dimensional, so that the flow variables are functions of one space coordinate only, corresponding variational principles associated with quasi one-dimensional shallow water flow can be derived from the two-dimensional versions given in [1]. This derivation is also described in Section 2.

In Section 3 consideration is given to variational principles for discontinuous shallow water flows. Under certain circumstances, when the outlet depth is specified to lie in a particular range of values, a hydraulic jump may occur in the flow. At such a point of discontinuity the differential equations which govern the flow are not applicable. The flow immediately in front of the jump is related to that immediately behind the jump by jump conditions which are statements of the governing physical laws at such discontinuities ([3]). Three jump conditions govern the flow at a discontinuity in shallow water. One condition is used to locate the position of the jump and the other two relate the flow variables either side of the jump. All three conditions may be incorporated in variational principles for discontinuous flows.

Approximations to continuous and discontinuous shallow water flows are sought using the derived functionals. The method used is to find functions in a prescribed finite dimensional space for which the functionals are stationary. In Section 4 finite dimensional expansions using finite element basis functions are substituted into the variational principles and used to derive approximations on a fixed grid to the flow variables in one and two dimensions.

Approximations to continuous flows on adaptive grids are also considered. The jump conditions, derived in Section 3 for discontinuous flows, can be applied to the approximate solution at the internal nodes of the grid to give an algorithm for generating grid dependent solutions. This process is given in Section 5. An alter-

native method, based on similar reasoning, but solving directly the requirement that the functionals are stationary with respect to variations in the positions of the grid points, is also given in Section 5. In the case of minimising a functional these two methods of generating grid dependent solutions should derive minimum values less than those derived for the solutions generated on fixed grids but still greater than the exact minimum. Similar remarks hold for the case of a maximum principle.

Attempts are also made to approximate discontinuous flows. Finite dimensional approximations can be calculated in regions of the domain away from the hydraulic jump using the variational principles for continuous flow and regarding the pre- and post-jump approximations as independent. The actual position of the hydraulic jump is found using the jump conditions. Details are given in Section 5.

2 Variational Principles for Continuous Flows

2.1 The Shallow Water Approximation

Shallow water theory is an approximation to free surface flow in circumstances where the depth of fluid is much less than some characteristic horizontal length scale of the motion. It is essentially a vertically averaged representation of the flow and reduces the problem to one which is two-dimensional in the horizontal coordinates.

Only flows of constant equilibrium depth are considered here.

Consider a domain D in the horizontal (x, y) plane. Let d be the depth of fluid and \mathbf{v} the velocity, both defined on D. Define the mass flow vector \mathbf{Q} by

$$\mathbf{Q} = d\mathbf{v} \tag{2.1}$$

and the energy E by

$$E = gd + \frac{1}{2}\mathbf{v}.\mathbf{v},\tag{2.2}$$

where g is the acceleration due to gravity. The shallow water equations of steady irrotational motion are given by

$$\nabla \cdot \mathbf{Q} = 0$$
 conservation of mass, (2.3)

$$\nabla E = \mathbf{0}$$
 conservation of momentum, (2.4)

$$\mathbf{v} = \nabla \phi \quad \text{irrotationality},$$
 (2.5)

where ϕ is a velocity potential defined on D and

$$\mathbf{\nabla} \equiv \left(\frac{\partial}{\partial x}, \frac{\partial}{\partial y} \right).$$

Details are given in Stoker [3]. The conservation of momentum equation (2.4) is satisfied by E = constant for continuous flows. Thus the energy E is considered to be a constant whose value is to be specified.

Let D be a channel of slowly varying breadth B(x) and consider a section of the channel occupying the interval $[x_e, x_o]$ of the x-axis. Then, under the above conditions, the flow can be assumed to be quasi one-dimensional in the x direction. The flow variables are functions of x alone. The ∇ operator is replaced by $\frac{1}{B(x)} \frac{d}{dx} (B(x) \cdot)$ and ∇ by $\frac{d}{dx}$. The quasi one-dimensional counterparts of (2.3) and (2.5) are

$$(BQ)' = 0$$
 conservation of mass, (2.6)

$$v = \phi', \tag{2.7}$$

where ' denotes $\frac{d}{dx}$. The one-dimensional version of the conservation of momentum equation, E' = 0, is satisfied exactly by the assumption that E is constant on $[x_e, x_o]$.

2.2 Variational Principles for Steady Shallow Water

In [1] the variational principle of Luke [2] for fluid with a free surface was used to derive four variational principles for unsteady shallow water flow by applying the shallow water approximation to the variables within the functional and performing changes of variables using (2.1) and (2.2). These principles were then reduced to corresponding principles for steady shallow water by assuming that all of the flow variables are independent of time. The resulting variational principles for steady shallow water are given by

$$\delta L_{1}(\mathbf{Q}, \mathbf{v}, \phi) = \delta \left\{ \iint_{D} \left(p(\mathbf{v}, E) + \mathbf{Q} \cdot (\mathbf{v} - \nabla \phi) \right) dx dy + \int_{\Sigma} C \phi d\Sigma \right\} = 0,$$

$$(2.8)$$

$$\delta L_2(\mathbf{Q}, d, \phi) = \delta \left\{ \iint_D \left(r(\mathbf{Q}, d) + Ed + \phi \mathbf{\nabla} \cdot \mathbf{Q} \right) dx \, dy + \int_{\Sigma} \phi \left(C - \mathbf{Q} \cdot \mathbf{n} \right) d\Sigma \right\} = 0, \tag{2.9}$$

$$\delta L_3(\mathbf{Q}, \phi) = \delta \left\{ \iint_D \left(P(\mathbf{Q}, E) + \phi \mathbf{\nabla} \cdot \mathbf{Q} \right) dx \, dy + \int_{\Sigma} \phi \left(C - \mathbf{Q} \cdot \mathbf{n} \right) d\Sigma \right\} = 0, \tag{2.10}$$

$$\delta L_4(\mathbf{Q}, d, \mathbf{v}, \phi) = \delta \left\{ \iint_D (-R(\mathbf{v}, d) + \mathbf{Q}.\mathbf{v} + Ed + \phi \mathbf{\nabla}.\mathbf{Q}) \, dx \, dy + \int_{\Sigma} \phi \left(C - \mathbf{Q}.\mathbf{n} \right) \, d\Sigma \right\} = 0.$$
 (2.11)

The function p is defined by

$$p(\mathbf{v}, E) = \frac{1}{2g} \left(E - \frac{1}{2} \mathbf{v} \cdot \mathbf{v} \right)^2$$

and has the values of pressure. The function r can be described as the Lagrangian density (see [1]) and is defined by

$$r(\mathbf{Q}, d) = \frac{1}{2} \frac{\mathbf{Q} \cdot \mathbf{Q}}{d} - \frac{1}{2} g d^2.$$

The function R can be called the Hamiltonian density and is defined by

$$R(\mathbf{v}, d) = \frac{1}{2}gd^2 + \frac{1}{2}d\mathbf{v}.\mathbf{v}.$$

Finally, the function P has the values of flow stress and $P(\mathbf{Q}, E)$ is defined by eliminating \mathbf{v} and d from the equations

$$P = \frac{1}{2}gd^2 + d\mathbf{v}.\mathbf{v}$$
, $\mathbf{Q} = d\mathbf{v}$ and $E = gd + \frac{1}{2}\mathbf{v}.\mathbf{v}$.

The function C in (2.8)–(2.11) is a given function on the boundary Σ of D and E is regarded as a given constant in these principles.

The natural conditions of (2.8)–(2.11) include the equations of steady shallow water motion (2.3) and (2.5) expressed variously in terms of d, \mathbf{v} , \mathbf{Q} , ϕ and E depending on the generating functional. The natural boundary condition of each of the principles is

$$\mathbf{Q}.\mathbf{n} = C \text{ on } \Sigma.$$

Equations (2.8)–(2.11) can be used to generate finite dimensional approximations to solutions of the shallow water equations. This is done by substituting finite expansions for the flow variables into the functionals L_1 , L_2 , L_3 and L_4 and finding the coefficients which cause them to be stationary with respect to variations within the finite space.

In this report a constrained version of the 'p' principle (2.8) will be used. A variational principle can be constrained by considering only variations which satisfy one or more of the natural conditions. The other natural conditions remain as natural conditions ([4]). The 'p' principle (2.8) is constrained to satisfy irrotationality by substituting $\mathbf{v} = \nabla \phi$ into the integrand. This yields

$$\delta \bar{L}_1(\phi) = \delta \left\{ \iint_D p(\mathbf{\nabla}\phi, E) \, dx \, dy + \int_{\Sigma} C\phi \, d\Sigma \right\} = 0 \tag{2.12}$$

which has as natural conditions the conservation of mass equation, expressed in terms of ϕ and E, in D and a boundary condition for the mass flow, expressed in terms of ϕ . Equation (2.12) will be used in Section 4 to generate a finite element approximation to the velocity potential ϕ .

2.3 Variational Principles for Quasi One-dimensional Steady Shallow Water

In the same way that variational principles for unsteady shallow water flows were derived from principles for free surface flows in [1] by making the shallow water approximation, the quasi one-dimensional approximation can be applied to (2.8)–(2.11) to give variational principles for quasi one-dimensional shallow water in a slowly varying channel as follows.

Let all of the flow variables be functions of x alone. Substitute Q = Q(x), d = d(x), v = v(x) and $\phi = \phi(x)$ for their two-dimensional counterparts in (2.8)–(2.11). Replace the operators by their one-dimensional versions, that is, replace $\nabla \cdot \mathbf{Q}$ by $\frac{1}{B}(BQ)'$ in (2.9)–(2.11) and $\nabla \phi$ by ϕ' in (2.8). Then the integration with respect to y can be performed. The function C, defined on Σ , is the value of \mathbf{Q} .n on the boundary of the two-dimensional domain. Assuming that there is no flow across the fixed, lateral sides of the channel, then $C \equiv 0$ on this part of the boundary. Therefore the function C need only be prescribed at the inlet and outlet boundaries and is the value of the mass flow at inlet and outlet. In the one-dimensional case the boundary condition at inlet C_e is given the constant value C. To satisfy conservation of mass, the boundary condition at outlet C_o is defined by $C_o = \frac{CB_e}{B_o}$ where $B_e = B(x_e)$ and $B_o = B(x_o)$. Using these values the boundary integrals in (2.8)–(2.11) can also be evaluated.

The variational principles for quasi one-dimensional flow are given by

$$\delta J_{1} = \delta \left\{ \int_{x_{e}}^{x_{o}} B(p(v, E) + Q(v - \phi')) dx + CB_{e}(\phi(x_{o}) - \phi(x_{e})) \right\} = 0, \quad (2.13)$$

$$\delta J_2 = \delta \left\{ \int_{x_e}^{x_o} B(r(Q, d) + Ed - Q\phi') \, dx + CB_e(\phi(x_o) - \phi(x_e)) \right\} = 0, \quad (2.14)$$

$$\delta J_3 = \delta \left\{ \int_{x_e}^{x_o} B(P(Q, E) - Q\phi') \, dx + C B_e \left(\phi(x_o) - \phi(x_e) \right) \right\} = 0, \tag{2.15}$$

$$\delta J_4 = \delta \left\{ \int_{x_e}^{x_o} B(-R(v,d) + Q(v - \phi') + Ed) \, dx + CB_e(\phi(x_o) - \phi(x_e)) \right\} = 0,$$
(2.16)

where $J_1 = J_1(Q, v, \phi)$, $J_2 = J_2(Q, d, \phi)$, $J_3 = J_3(Q, \phi)$ and $J_4 = J_4(Q, d, v, \phi)$. The natural conditions of (2.13)–(2.16) in the domain $[x_e, x_o]$ include the conservation of mass equation (2.6) and equation (2.7), expressed in different variables depending on the generating functional. The natural boundary conditions, common to all of (2.13)–(2.16), are

$$(QB)|_{x_e} = CB_e \text{ and } (QB)|_{x_o} = CB_e.$$
 (2.17)

Equations (2.13)-(2.16) can be used to generate finite element approximations to quasi one-dimensional shallow water flows in the same way as for the two-dimensional equations. Constrained versions of the 'p' principle (2.13) and the 'r' principle (2.14) are now considered.

Following the derivation of the constrained two-dimensional 'p' principle (2.12), the variations in (2.13) are constrained to satisfy the natural condition $v = \phi'$. This yields the variational principle

$$\delta \bar{J}_{1}(\phi) = \delta \left\{ \int_{x_{e}}^{x_{o}} Bp(\phi', E) \, dx + CB_{e} \left(\phi(x_{e}) - \phi(x_{o}) \right) \right\} = 0$$
 (2.18)

which has as its only natural condition in $[x_e, x_o]$ the conservation of mass equation (2.6), expressed in term of ϕ , and boundary conditions for ϕ .

The 'r' principle (2.14) is constrained to satisfy conservation of mass, (QB)' = 0, in $[x_e, x_o]$. For consistency the natural conditions (2.17) must also be applied as constraints. The constrained 'r' principle is given by

$$\delta \bar{J}_2(d) = \delta \left\{ \int_{x_e}^{x_o} B\left(r(Q, d) + Ed\right) dx \right\} = 0 \tag{2.19}$$

where $Q(x) = \frac{CB_e}{B(x)}$ in $[x_e, x_o]$.

The functionals in (2.18) and (2.19) each depend on only one variable and will be used in Section 4 to generate approximations to the velocity potential and the depth of flow respectively. The unconstrained 'r' principle (2.14) depends on Q, d and ϕ and will be used to give approximations to all three variables.

3 Discontinuous Flows and Variational Principles

The variational principles of Sections 2.2 and 2.3 are all concerned with continuous flows. In this section variational principles for quasi one-dimensional flows with hydraulic jumps are considered.

Hydraulic jumps may occur when conditions are imposed on the flow at the outlet boundary which cannot be achieved by a continuous flow. The value of the energy E, defined by (2.2), is not conserved at a hydraulic jump, although values of mass flow Q and flow stress P are ([3]). These conditions are known as jump conditions and are explicitly given by

$$[Q]_{x_s} = 0, [P]_{x_s} = 0 \text{ and } [E]_{x_s} > 0$$
 (3.1)

where the brackets $[\cdot]_{x_s}$ denote the jump in the value of the quantity at the point x_s . That is, for example, $[Q]_{x_s} = Q|_{x_{s+}} - Q|_{x_{s-}}$ where + denotes the inlet side of the jump position and - denotes the outlet side of the jump position.

The property $[E]_{x_s} \neq 0$ is used in the method to approximate discontinuous solutions as, in the variational principles, the constant E may be assigned one value in the channel before the hydraulic jump and another, smaller value behind the jump. The value at inlet, E^e , must be specified. A value at outlet, E^o , which forces the flow to be discontinuous can be calculated from the outlet boundary condition. In this report a value of the depth at outlet, d_o , will be specified. Using conservation of mass, the value of mass flow at outlet can be calculated as $Q_o = \frac{CB_e}{B_o}$. The definition of mass flow (2.1) then yields the value of the velocity at outlet, that is, $v_o = \frac{Q_o}{d_o}$. Then the outlet energy can be calculated, using (2.2), as $E^o = gd_o + \frac{1}{2}v_o^2$.

Equations (2.6) and (2.7) govern the motion in the channel away from the jump but at the discontinuity, where derivatives are not defined, the differential equations do not apply. The behaviour of the flow variables at a point of discontinuity is governed by the jump conditions (3.1), two of which can be derived as the natural conditions of variational principles for quasi one-dimensional flow as follows.

Consider first a general functional of the form

$$I(x_s, \mathbf{u}) = \int_{x_e}^{x_s} F(x, \mathbf{u}, \mathbf{u}') dx + \int_{x_s}^{x_o} F(x, \mathbf{u}, \mathbf{u}') dx + [g(x, \mathbf{u})]_{x_e}^{x_o}$$
(3.2)

where $\mathbf{u} = (u_1(x), \dots, u_n(x))^T$, $\mathbf{u}' = (u_1'(x), \dots u_n'(x))^T$ and $x_s \in (x_e, x_o)$ is a point at which any of the u_i may be discontinuous. The position of x_s is allowed to vary in the variational principle $\delta I = 0$ and gives rise to jump conditions. Using Taylor series $\delta I = 0$ gives

$$\int_{x_{e}}^{x_{s}} \sum_{i=1}^{n} \left\{ F_{u_{i}} - F_{u_{i}'x} - \sum_{j=1}^{n} \left(F_{u_{i}'u_{j}} u_{j}' + F_{u_{i}'u_{j}'} u_{j}'' \right) \right\} \delta u_{i} dx
+ \int_{x_{s}}^{x_{o}} \sum_{i=1}^{n} \left\{ F_{u_{i}} - F_{u_{i}'x} - \sum_{j=1}^{n} \left(F_{u_{i}'u_{j}} u_{j}' + F_{u_{i}'u_{j}'} u_{j}'' \right) \right\} \delta u_{i} dx
+ \sum_{i=1}^{n} \left(F_{u_{i}'} + g_{u_{i}} \right) \delta u_{i}|_{x_{o}} - \sum_{i=1}^{n} \left(F_{u_{i}'} + g_{u_{i}} \right) \delta u_{i}|_{x_{e}}
+ \sum_{i=1}^{n} \left(F_{u_{i}'} \delta u_{i}|_{x_{s+}} - F_{u_{i}'} \delta u_{i}|_{x_{s-}} \right) + \delta x_{s} \left(F|_{x_{s+}} - F|_{x_{s-}} \right) = 0, \quad (3.3)$$

where x_{s+} is the side of the point x_{s} towards x_{e} and x_{s-} is the side of x_{s} towards x_{o} . At the point x_{s} , the total variation in u_{i} is given by $\delta u_{i}\big|_{x_{s}} = \delta u_{i}\big|_{x_{s}} + u'_{i}(x_{s})\delta x_{s}$. Substituting this into (3.3) gives the natural conditions of $\delta I = 0$ as follows.

$$\delta u_i$$
: $F_{u_i} - \frac{d}{dx} F_{u'_i} = 0$ $i = 1, ..., n$ $x \in [x_e, x_s) \cup (x_s, x_o].$ (3.4)

$$\delta u_i|_{x_o} : \left(F_{u_i'} + g_{u_i} \right)|_{x_o} = 0 \ i = 1, \dots, n.$$
 (3.5)

$$\delta u_i|_{x_e} : \left(F_{u_i'} + g_{u_i} \right)|_{x_e} = 0 \ i = 1, \dots, n.$$
 (3.6)

$$\hat{\delta u_i}\Big|_{x_s}$$
: $\left[F_{u_i'}\right]_{x_s} = 0$ $i = 1, \dots, n.$ (3.7)

$$\delta x_s : \left[F - \sum_{i=1}^n F_{u'_i} u'_i \right]_{x_s} = 0.$$
 (3.8)

The functionals in the one-dimensional variational principles (2.13)–(2.16) are all of the form (3.2) with Q, d, v and ϕ being identified with the u_i as appropriate. Thus the natural conditions of (2.13)–(2.16) are given by (3.4)–(3.8). The natural conditions caused by variations of the u_i in the domain, (3.4), and on the inlet and outlet boundaries, (3.5) and (3.6), are the same as those for the continuous

case in Section 2.2. In addition, there are jump conditions caused by the variation of x_s , given by,

```
for the 'p' principle [BQ]_{x_s} = 0 and [B(p(v, E) + Qv)]_{x_s} = 0,
for the 'r' principle [BQ]_{x_s} = 0 and [B(r(Q, d) + Ed)]_{x_s} = 0,
for the 'P' principle [BQ]_{x_s} = 0 and [BP(Q, E)]_{x_s} = 0 and
for the 'R' principle [BQ]_{x_s} = 0 and [B(-R(v, d) + Qv + Ed)]_{x_s} = 0.
```

The first jump condition in each case is the conservation of mass flow across the discontinuity since, by hypothesis for quasi one-dimensional flow, the breadth B is continuous. The same argument applies to the second jump condition in each case which states that there is no change in the value of the flow stress P across the jump. That the conditions are the same can be seen by using the definitions of mass flow and energy, (2.1) and (2.2), to perform changes of variables.

The conditions $[Q]_{x_s} = 0$ and $[P]_{x_s} = 0$ are the same as $(3.1)_1$ and $(3.1)_2$ and are consistent with the theory ([3]).

The constrained 'r' principle (2.19) will be considered for practical implementation. The functional for this case is

$$I_1(d) = \int_{x_e}^{x_s} B(r(Q, d) + E^e d) dx + \int_{x_s}^{x_o} B(r(Q, d) + E^o d) dx$$
 (3.9)

where $Q = \frac{CB_e}{B}$. The natural jump condition of $\delta I_1 = 0$ is

$$(r(Q,d) + E^e d)|_{x_{s+}} - (r(Q,d) + E^o d)|_{x_{s-}} = 0.$$
(3.10)

One method of generating approximations to discontinuous depth functions which will be given in Section 5 involves finding continuous solutions on $[x_e, x_s)$ and $(x_s, x_o]$, with x_s fixed, and coupling them at the point x_s using the jump condition (3.10).

It is possible to define any number of points like x_s in the domain $[x_e, x_o]$ thus splitting it into several intervals. If the positions of all of these points are allowed to vary then the one-dimensional variational principles yield the two jump conditions $[BQ]_{x_s} = 0$ and $[BP]_{x_s} = 0$ at each of these points. This gives a basis for a method to generate solutions on adaptive grids which is implemented in Section 5.

4 Approximations on Fixed Grids

Finite element expansions are now used to generate approximate solutions of the shallow water equations for flows in channels with horizontal beds. In this section methods are considered for calculating approximations on fixed grids. The algorithms are intended only for generating approximations to continuous solutions since a hydraulic jump would be poorly approximated unless it occurred at a grid point.

4.1 Approximate Quasi One-dimensional Flows

In this section methods will be developed to calculate quasi one-dimensional approximations to the shallow water equations using three of the variational principles of Section 2 — (2.14), (2.18) and (2.19). The constrained 'r' principle (2.19) involves a functional of the variable d, the fluid depth, alone and is used to generate an approximation to d.

4.1.1 The Constrained 'r' Principle

Let the domain $[x_e, x_o]$ be divided into n-1 intervals by the set of points x_i (i = 1, ..., n). The finite element approximation d^h , to the depth function d, is defined on this grid by

$$d^{h}(x) = \sum_{i=1}^{n} d_{i}\alpha_{i}(x), \tag{4.1}$$

where the α_i (i = 1, ..., n) are finite element basis functions and the d_i (i = 1, ..., n) are the coefficients of the approximation at the grid points x_i .

The finite element approximation to d is defined to be the function for which the constrained 'r' functional, \bar{J}_2 in (2.19), is stationary within the space spanned by the set of basis functions. Let

$$L_1(\mathbf{d}) = \int_{x_1}^{x_n} B\left(r(Q, d^h) + Ed^h\right) dx \tag{4.2}$$

where $Q(x) = \frac{CB_e}{B(x)}$, d^h is given by (4.1) and $\mathbf{d} = (d_1, \dots, d_n)^T$. The finite element solution is such that L_1 is stationary with respect to variations in \mathbf{d} , that is,

$$F_{j}(\mathbf{d}) = \frac{\partial L_{1}}{\partial d_{j}} = \int_{x_{1}}^{x_{n}} B(r_{d^{h}} + E) \alpha_{j} dx = 0 \quad j = 1, \dots, n.$$
 (4.3)

This system of equations can be solved using Newton's method. The Jacobian, J, is given by

$$J(\mathbf{d}) = \{J_{ij}\} = \left\{\frac{\partial F_i}{\partial d_j}\right\} = \left\{\frac{\partial^2 L_1}{\partial d_i \partial d_j}\right\} = \left\{\int_{x_1}^{x_n} Br_{d^h d^h} \alpha_i \alpha_j \, dx\right\}$$
(4.4)

and is the Hessian of L_1 .

Given an approximation, \mathbf{d}^k , to the solution \mathbf{d} a hopefully more accurate approximation, \mathbf{d}^{k+1} , is found using Newton's method, that is,

$$\mathbf{d}^{k+1} = \mathbf{d}^k + \delta \mathbf{d}^k, \tag{4.5}$$

where
$$J\left(\mathbf{d}^{k}\right)\delta\mathbf{d}^{k} = -\mathbf{F}\left(\mathbf{d}^{k}\right).$$
 (4.6)

The process is repeated until

$$\max_{i} \left| \delta d_i^k \right| < \text{ tolerance.} \tag{4.7}$$

The Jacobian, J, and the vector $\mathbf{F} = (F_1, \dots, F_n)^T$ are evaluated using the seven point Gaussian quadrature formula.

It is possible to deduce properties of the expected solutions using the fact that the Jacobian is the Hessian of L_1 . From the definition of the function $r(\mathbf{Q}, d)$ in Section 2.2, the second derivative of $r(Q, d^h)$ is given by

$$r_{d^h d^h} = \frac{Q^2}{d^{h^3}} - g. (4.8)$$

Substituting the definitions $Q = d^h v^h$ and $v^{h^2} = 2(E - gd^h)$ into (4.8) gives

$$r_{d^h d^h} = \frac{2E}{d^h} - 3g. (4.9)$$

The depth approximation d^h is termed critical at a point if $d^h = \frac{2E}{3g}$. This is in agreement with the definition of critical flow in the exact solutions and corresponds to a point where the velocity has the critical value $c_* = \sqrt{gd}$. From (4.9) it can be seen that if the flow is subcritical, that is $d^h > \frac{2E}{3g}$, then $r_{d^hd^h} < 0$ and if the flow is supercritical, that is $d^h < \frac{2E}{3g}$, then $r_{d^hd^h} > 0$. From (4.4) the Jacobian has the form of a weighted mass matrix, where $Br_{d^hd^h}$ is the weight function. Thus if the approximated flow is subcritical in the domain throughout the iterations J is negative definite and the solution of (4.3) maximises L_1 . Alternatively, if the iterated approximate flow is supercritical in the whole domain J is positive definite and the solution of (4.3) minimises L_1 . If both subcritical and supercritical flow occur during the iterations then J may be indefinite.

Thus, given the energy, E, of the flow, the mass flow at channel inlet, C, and the breadth variation of the channel B(x), finite element depth solutions can be generated for continuous flows which are either wholly subcritical or wholly supercritical in the domain except for a possible region of critical flow.

The algorithm is implemented on the equi-spaced grid given by

$$x_i = x_e + \frac{i-1}{n-1}(x_o - x_e)$$
 $i = 1, ..., n,$ (4.10)

where $x_e = 0$, $x_o = 10$ and n = 21. Two sets of basis functions are considered: the first, α_i^l (i = 1, ..., n), leads to continuous piecewise linear approximations and the second, α_i^c (i = 1, ..., n - 1), gives discontinuous piecewise constant approximations. The basis functions are defined by

$$\alpha_{1}^{l}(x) = \begin{cases} \frac{x_{2}-x}{x_{2}-x_{1}} & x \in [x_{1}, x_{2}] \\ 0 & x \notin [x_{1}, x_{2}] \end{cases},$$

$$\alpha_{i}^{l}(x) = \begin{cases} \frac{x-x_{i-1}}{x_{i}-x_{i-1}} & x \in [x_{i-1}, x_{i}] \\ \frac{x_{i+1}-x}{x_{i+1}-x_{i}} & x \in [x_{i}, x_{i+1}] \\ 0 & x \notin [x_{i-1}, x_{i+1}] \end{cases} \qquad i = 2, \dots, n-1, \qquad (4.11)$$

$$\alpha_{n}^{l}(x) = \begin{cases} \frac{x-x_{n-1}}{x_{n}-x_{n-1}} & x \in [x_{n-1}, x_{n}] \\ 0 & x \notin [x_{n-1}, x_{n}] \end{cases},$$

and

$$\alpha_i^c(x) = \begin{cases} 1 & x \in (x_i, x_{i+1}) \\ 0 & x \notin (x_i, x_{i+1}) \end{cases} \qquad i = 1, \dots, n-1, \tag{4.12}$$

and are shown in Figure 1.

For the basis functions defined by (4.11), J is tridiagonal and (4.6) is solved quickly for $\delta \mathbf{d}^k$ using Gaussian elimination and back substitution. For the basis functions defined by (4.12), J is diagonal and (4.6) is easily solved.

The energy, E, of the flow is taken to be 50 which gives a critical depth of $d_* = \frac{100}{30} \simeq 3.33$. Two values of the mass flow at inlet, C, are used. One value is given by $C = \frac{Q_*B_*}{B_e}$ where Q_* is the critical mass flow $Q_* = \frac{1}{g} \left(\frac{2E}{3}\right)^{\frac{3}{2}}$ and B_* is the breadth of the channel at the point where B'(x) = 0 and the breadth is a minimum — the channel throat. This generates approximations to flows which are critical at the channel throat. Non-critical flows are approximated by specifying C to be less than $\frac{Q_*B_*}{B_*}$.

Several breadth functions are considered. These are

$$B_1(x) = 6 + 4\left(1 - \frac{x}{\left(\frac{x_e + x_o}{2}\right)}\right)^k \qquad x \in [x_e, x_o], \quad k = 2, 4, 8, \quad (4.13)$$

$$B_2(x) = 6 + 4 \left| 1 - \frac{x}{\left(\frac{x_e + x_o}{2}\right)} \right| \qquad x \in [x_e, x_o], \tag{4.14}$$

$$B_3(x) = \begin{cases} 6+4\left(1-\left(\frac{x-x_e}{\nu-x_e}\right)^{\sigma}\right) & x \in [x_e, \nu] \\ 6+4\left(1-\left(\frac{x_o-x}{x_o-\nu}\right)^{\sigma}\right) & x \in [\nu, x_o] \end{cases}$$
(4.15)

For these breadth distributions the value of C yielding critical flows is 11.5; the value C = 10 is used to give examples of non-critical flows.

The tolerance on the Newton iteration in (4.7) is taken to be 10^{-3} .

The initial approximation, \mathbf{d}^0 , to the solution \mathbf{d} affects whether the converged finite element solution is an approximation to subcritical or supercritical flow. In practice subcritical solutions are obtained by specifying $d_i^0 > d_*$ (i = 1, ..., n) and supercritical solutions are obtained by specifying $d_i^0 < d_*$ (i = 1, ..., n).

Using the piecewise linear basis functions (4.11) and the breadth distribution $B_1(x)$ (k=2), Newton's method converges to the supercritical solution from the initial approximation $d_i^0 = 1$ ($i=1,\ldots,n$) in 11 iterations for critical flow and in 5 iterations for non-critical flow. Subcritical solutions are obtained, using $d_i^0 = 4$ ($i=1,\ldots,n$), in 6 iterations for critical flow and 3 iterations for non-critical flow.

With the piecewise constant basis functions (4.12) and the breadth distribution $B_1(x)$ (k = 2), the supercritical solution, using $d_i^0 = 1$ (i = 1, ..., n), is found after 10 iterations for critical flow and 5 iterations for non-critical flow while the

subcritical solution, using $d_i^0 = 4$ (i = 1, ..., n), is found after 5 iterations for critical flow and 3 iterations for non-critical flow.

Figure 2a shows the finite element depth approximations for critical and noncritical flows in a channel with breadth distribution $B_1(x)$ (k = 8). The top two solutions are approximations to subcritical flows and the other two approximate supercritical flows. Figure 2b shows a linear interpolation to the breadth function using the 21 grid points given by (4.10). The sides of the channel are almost parallel for much of its length where the breadth is smallest so the depths of the critical flows are close to the critical value for some distance around the point x = 5.

Figure 3a shows the finite element approximations for the breadth distribution $B_3(x)$ where $\nu = 7.5$ and $\sigma = 1.5$. The linear interpolation of the breadth function is given in Figure 3b. The depth approximations are critical in value only at the point of the channel throat, that is, at x = 7.5.

If the components of the initial approximation \mathbf{d}^0 are close to the value of the critical depth d_* then it is possible that the Jacobian may become indefinite during the iteration and Newton's method may not converge. The method may also fail when approximating certain critical flows. This is due to the subcritical and supercritical solutions being close together in a region of near-critical flow. In this case, for a subcritical approximation the iteration process may calculate the supercritical solution at nodes near the channel throat. This causes the Jacobian to become indefinite. One way to prevent this is to reassign any supercritical values to be slightly subcritical, then the Jacobian remains negative definite. The supercritical approximation to a critical flow may need a similar adjustment.

Thus finite element approximations to quasi one-dimensional depth variations in a channel can be calculated using the constrained 'r' principle (2.19). The algorithm is now applied to the constrained 'p' principle (2.18) to generate piecewise linear approximations to the velocity potential.

4.1.2 The Constrained 'p' Principle

The algorithm of the previous section is applied to the quasi one-dimensional 'p' principle, constrained to satisfy $v = \phi'$, (2.18).

The domain is divided into n-1 intervals, by the points x_i $(i=1,\ldots,n)$, as before. The x_i are defined by (4.10). The finite element approximation to the velocity potential ϕ is given by

$$\phi^h(x) = \sum_{i=1}^n \phi_i \alpha_i(x), \tag{4.16}$$

where the α_i (i = 1, ..., n) are the piecewise linear basis functions (4.11) and the ϕ_i (i = 1, ..., n) are the values of the finite element approximation at the grid

points x_i .

Let

$$L_2(\phi) = \int_{x_1}^{x_n} Bp(\phi^{h'}, E) dx + CB_e \left(\phi^h(x_n) - \phi^h(x_1)\right)$$
(4.17)

where $\phi = (\phi_1, \dots, \phi_n)^T$. The finite element approximation to the velocity potential is given by ϕ such that $L_2(\phi)$ is stationary, that is,

$$F_i(\phi) = \frac{\partial L_2}{\partial \phi_i} = \int_{x_1}^{x_n} B p_{\phi^{h'}} \alpha_i{'} dx + C B_e \left(\alpha_i(x_n) - \alpha_i(x_1) \right) = 0 \ i = 1, \dots, n. \ (4.18)$$

The solution is found using Newton's method. The Jacobian, J, is given by

$$J(\phi) = \{J_{ij}\} = \left\{\frac{\partial F_i}{\partial \phi_j}\right\} = \left\{\frac{\partial^2 L_2}{\partial \phi_i \partial \phi_j}\right\} = \left\{\int_{x_1}^{x_n} B p_{\phi^{h'} \phi^{h'}} \alpha_i' \alpha_j' dx\right\}$$

and is the Hessian of L_2 . As for the 'r' principle, the Jacobian can be used to give information about the approximations. From the definition of the function $p(\mathbf{v}, E)$, the second derivative of $p(\phi^{h'}, E)$ is given by

$$p_{\phi^{h'}\phi^{h'}} = \frac{1}{g} \left(\frac{3}{2} \left(\phi^{h'} \right)^2 - E \right).$$

Using the constraint $v=\phi'$, an approximation, v^h , to the velocity, v, is given by $v^h=\phi^{h'}$. The critical speed c_* is defined by $c_*=\sqrt{\frac{2E}{3}}$ so that subcritical solutions, with $v^h< c_*$, have $p_{\phi^{h'}\phi^{h'}}<0$ and supercritical solutions, with $v^h>c_*$, have $p_{\phi^{h'}\phi^{h'}}>0$. Thus, for subcritical flows J is negative definite and for supercritical flows J is positive definite.

Given an approximation, ϕ^k , to the solution ϕ a hopefully more accurate approximation, ϕ^{k+1} , is given by Newton's method, that is,

$$\boldsymbol{\phi}^{k+1} = \boldsymbol{\phi}^k + \delta \boldsymbol{\phi}^k, \tag{4.19}$$

where
$$J\left(\phi^{k}\right)\delta\phi^{k} = -\mathbf{F}\left(\phi^{k}\right)$$
. (4.20)

The process is repeated until

$$\max_{i} \left| \delta \phi_i^k \right| < \text{ tolerance.} \tag{4.21}$$

The Jacobian and the vector \mathbf{F} are integrated exactly. The Jacobian is again tridiagonal and (4.20) is solved by Gaussian elimination and back substitution.

The initial approximation, ϕ^0 , to the velocity potential is given by

$$\phi_i^0 = \frac{i-1}{n-1} v_0 \quad i = 1, \dots, n$$
 (4.22)

where v^0 is assigned a value which determines whether the solution being calculated will be the subcritical or the supercritical approximation. If $v^0 < c_* \frac{x_o - x_e}{n-1}$ the solution will be subcritical and if $v^0 > c_* \frac{x_o - x_e}{n-1}$ the solution will be supercritical.

The algorithm is implemented on the grid given by (4.10) where $x_e = 0$, $x_o = 10$ and n = 21. The energy E is again taken to be 50. Approximations to flows in channels with breadth distributions given by (4.13)–(4.15) are considered. The two values of mass flow at inlet C = 11.5 and C = 10 are used to generate critical and non-critical approximations.

Using $B_1(x)$ (k=2) and with a tolerance on the Newton iteration of 10^{-3} the method converges to the subcritical solution in 4 iterations using $v^0 = 2$ and to the supercritical solution in 4 iterations using $v^0 = 4$ for non-critical flows. For critical flows the method converges to the subcritical solution in 6 iterations using $v^0 = 2$ and to the supercritical solution in 7 iterations using $v^0 = 4$.

Results for the quadratic channel breadth case are shown in Figure 4. The approximations are for supercritical flow which is critical at the channel throat. Figure 4a is the linear interpolation of the breadth function at the 21 grid points. Figure 4b is a piecewise constant approximation to the velocity, calculated using $v^h = \phi^{h'}$ on each element. Figure 4c is the piecewise linear approximation to the velocity potential.

Thus the constrained 'p' principle (2.18) can be used to calculate a piecewise linear approximation to the velocity potential and hence a piecewise constant velocity approximation.

4.1.3 The Unconstrained 'r' Principle

The algorithm used in Sections 4.1.1 and 4.1.2 is now extended and applied to the quasi one-dimensional unconstrained 'r' principle (2.14) to generate piecewise linear approximations to depth, velocity potential and mass flow.

The approximations are defined on the grid given by (4.10) with $x_e = 0$, $x_o = 10$ and n = 41. They are

$$Q^{h}(x) = \sum_{i=1}^{n} Q_{i}\alpha_{i}(x) , d^{h}(x) = \sum_{i=1}^{n} d_{i}\alpha_{i}(x) , \phi^{h}(x) = \sum_{i=1}^{n} \phi_{i}\alpha_{i}(x) , \qquad (4.23)$$

where the α_i (i = 1, ..., n) are the piecewise linear basis functions (4.11). The approximations (4.23) are substituted into the functional for the discrete version of the 'r' principle (2.14), given by,

$$L_3(\mathbf{Q}, \mathbf{d}, \boldsymbol{\phi}) = \int_{x_1}^{x_n} B\left(r(Q^h, d^h) + Ed^h - \phi^{h'}Q^h\right) dx + CB_e\left(\phi^h(x_n) - \phi^h(x_1)\right)$$

$$(4.24)$$

where $\mathbf{Q} = (Q_1, \dots, Q_n)^T$, $\mathbf{d} = (d_1, \dots, d_n)^T$ and $\boldsymbol{\phi} = (\phi_1, \dots, \phi_n)^T$. The approximate solutions are generated using the values of \mathbf{Q} , \mathbf{d} and $\boldsymbol{\phi}$ such that

$$\frac{\partial L_3}{\partial d_i} = 0 , \quad \frac{\partial L_3}{\partial Q_i} = 0 , \quad \frac{\partial L_3}{\partial \phi_i} = 0 \quad i = 1, \dots, n.$$
 (4.25)

Equations $(4.25)_3$ yield

$$-\int_{x_1}^{x_n} B\alpha_i' Q^h \, dx + CB_e \left(\alpha_i(x_n) - \alpha_i(x_1)\right) = 0 \quad i = 1, \dots, n,$$

which may be rewritten as

$$\sum_{j=1}^{2} Q_{j} \int_{x_{1}}^{x_{2}} B\alpha_{1}' \alpha_{j} dx = -CB_{e},$$

$$\sum_{j=i-1}^{i+1} Q_{j} \int_{x_{i-1}}^{x_{i+1}} B\alpha_{i}' \alpha_{j} dx = 0 \qquad i = 2, \dots, n-1,$$

$$\sum_{j=n-1}^{n} Q_{j} \int_{x_{n-1}}^{x_{n}} B\alpha_{n}' \alpha_{j} dx = CB_{e},$$

or as

$$A_Q \mathbf{Q} = \mathbf{C}_Q, \tag{4.26}$$

where A_Q is a constant $n \times n$ matrix and \mathbf{C}_Q is a constant $n \times 1$ vector with only first and last entries non-zero. The matrix A_Q is of rank n-1 and is singular but, using the boundary condition $Q_1 = C$, the solution of (4.26) is unique. A_Q is tridiagonal so \mathbf{Q} is calculated using Gaussian elimination and back substitution.

Equations $(4.25)_1$ yield

$$\int_{x_1}^{x_n} B(r_{d^h} + E) \alpha_i dx = 0 \quad i = 1, \dots, n$$

which, once Q^h is known, can be solved for d^h in the same way as in Section 4.1.1. Equations $(4.25)_2$ give

$$\int_{x_1}^{x_n} B\left(r_{Q^h} - \phi^{h'}\right) \alpha_i \, dx = 0 \quad i = 1, \dots, n,$$

which may be rewritten as

$$\sum_{j=1}^{2} \phi_{j} \int_{x_{1}}^{x_{2}} B\alpha_{1} \alpha_{j}' dx = \int_{x_{1}}^{x_{2}} Br_{Q^{h}} \alpha_{1} dx,$$

$$\sum_{j=i-1}^{i+1} \phi_{j} \int_{x_{i-1}}^{x_{i+1}} B\alpha_{i} \alpha_{j}' dx = \int_{x_{i-1}}^{x_{i+1}} Br_{Q^{h}} \alpha_{i} dx \quad i = 2, \dots, n-1,$$

$$\sum_{j=n-1}^{n} \phi_{j} \int_{x_{n-1}}^{x_{n}} B\alpha_{n} \alpha_{j}' dx = \int_{x_{n-1}}^{x_{n}} Br_{Q^{h}} \alpha_{n} dx,$$

or as

$$A_{\phi}\phi = \mathbf{C}_{\phi}$$

where A_{ϕ} is an $n \times n$ matrix and \mathbf{C}_{ϕ} is an $n \times 1$ vector. Once ϕ^h and d^h are known ϕ can be calculated directly. The matrix A_{ϕ} is of rank n-1 and singular but ϕ is a potential function and the important quantity is its gradient so one of the values, say ϕ_1 , can be specified arbitrarily. This procedure is equivalent to setting the arbitrary constant in ϕ by assigning its value at the boundary.

Results for critical flow in a channel with breadth $B_1(x)$ (k = 4), given by (4.13), are shown in Figure 5. The energy E is taken to be 50. The piecewise linear approximation to mass flow is given in Figure 5a. The piecewise linear approximations to the velocity potential and depth for a supercritical flow are given in Figures 5b and 5c respectively. Figure 5d shows an approximation to the velocity, the height of each dot representing the magnitude of the velocity over a particular element.

Results for the corresponding subcritical flow are given in Figure 6.

Thus the quasi one-dimensional variational principles of Section 2 can be used to generate finite element approximations to all the variables of shallow water motion. The methods developed so far in this section are now extended to give an algorithm for generating such approximations in two-dimensions.

4.2 Approximate Two-dimensional Flows

The methods of Section 4.1 are extended and used on the constrained 'p' principle (2.12) to generate two-dimensional approximations to the velocity potential. The approach is essentially the same as the one-dimensional method.

The domain in two dimensions is approximated by a triangular grid. The finite element approximation ϕ^h to the velocity potential is given by

$$\phi^{h}(x,y) = \sum_{i=1}^{p} \phi_{i} \beta_{i}(x,y)$$
 (4.27)

where the β_i $(i=1,\ldots,p)$ are two-dimensional finite element basis functions defined on the triangular grid and the ϕ_i $(i=1,\ldots,p)$ are the coefficients of the solution.

Let the domain for the discrete version of the constrained 'p' principle (2.12) be D^h , the region covered by the triangular grid. Consider the functional

$$L_4(\phi) = \iint_{D^h} p\left(\nabla \phi^h, E\right) dx dy + \int_{\Sigma_e} C\phi^h d\Sigma + \int_{\Sigma_o} C\phi^h d\Sigma,$$

where $\phi = (\phi_1, \dots, \phi_p)^T$ and Σ_e and Σ_o are the inlet and outlet boundaries of D^h . The finite element solution is defined by the ϕ which is such that L_4 is stationary with respect to variations in ϕ , that is,

$$F_i(\boldsymbol{\phi}) = \frac{\partial L_4}{\partial \phi_i} = \iint_{D^h} p_{\boldsymbol{\nabla}_{\phi^h}} \cdot \boldsymbol{\nabla} \beta_i \, dx \, dy + \int_{\Sigma_e} C \beta_i \, d\Sigma + \int_{\Sigma_e} C \beta_i \, d\Sigma = 0 \quad i = 1, \dots, p.$$

The solution can be found by Newton's method in the same way as before. The Jacobian is given by

$$J(\phi) = \{J_{ij}\} = \left\{\frac{\partial F_i}{\partial \phi_j}\right\} = \left\{\frac{\partial^2 L_4}{\partial \phi_i \partial \phi_j}\right\} = \left\{\iint_{D^h} \nabla \beta_j . p_{\nabla_{\phi^h} \nabla_{\phi^h}} . \nabla \beta_i \, dx \, dy\right\}.$$

Given an approximation, ϕ^k , to the solution ϕ a hopefully better approximation, ϕ^{k+1} , is given by Newton's method, that is,

$$\boldsymbol{\phi}^{k+1} = \boldsymbol{\phi}^k + \delta \boldsymbol{\phi}^k, \tag{4.28}$$

where
$$J(\phi^k)\delta\phi^k = -\mathbf{F}(\phi^k)$$
. (4.29)

The process is repeated until

$$\max_{i} \left| \delta \phi_i^k \right| < \text{tolerance.} \tag{4.30}$$

The channels used for illustration are all symmetric about the x-axis so that only one half of them need be considered. This does not affect the specification of the boundary function C since the symmetry implies that there is no mass flow across the axis of symmetry.

The triangular grid for each domain is defined using the grid points

$$x_{i+(j-1)n} = \frac{i-1}{n-1}(x_o - x_e) + x_e \quad i = 1, \dots, n, \ j = 1, \dots, m,$$

$$y_{i+(j-1)n} = \frac{1}{2} \frac{j-1}{m-1} B\left(x_{i+(j-1)n}\right) \quad i = 1, \dots, n, \ j = 1, \dots, m,$$

where p = mn. An example of a grid for n = 9 and m = 7 is given in Figure 7.

The finite element basis functions are defined on a triangular grid. The basis function corresponding to a particular node is piecewise linear over each element surrounding a node, of magnitude one at the node, zero at all other nodes (see Figure 8). Using these basis functions the integrands of the Jacobian and the vector $\mathbf{F} = (F_1, \dots, F_p)^T$ are constants over each element of the grid, so the Jacobian and \mathbf{F} are integrated exactly.

The Jacobian for Newton's iteration is no longer tridiagonal, as it was for the one-dimensional case. However equation (4.29) may still be solved efficiently for $\delta \phi^k$ using a pre-conditioned conjugate gradient method [5]. The Jacobian J is pre-conditioned by its diagonal entries, that is, by the matrix $P = \text{diag}(J_{11}, \ldots, J_{pp})$. The system

$$P^{-1}\left(\boldsymbol{\phi}^{k}\right)J\left(\boldsymbol{\phi}^{k}\right)P^{-1}\left(\boldsymbol{\phi}^{k}\right)\delta\boldsymbol{\psi}^{k}=-P^{-1}\left(\boldsymbol{\phi}^{k}\right)\mathbf{F}\left(\boldsymbol{\phi}^{k}\right)$$

is solved for $\delta \psi^k$ by the conjugate gradient method. Then the solution $\delta \phi^k$ is given by

$$\delta \boldsymbol{\phi}^k = P^{-1} \left(\boldsymbol{\phi}^k \right) \delta \boldsymbol{\psi}^k.$$

The effect of this pre-conditioning is to improve the convergence rate of the conjugate gradient iteration ([6]).

The algorithm is implemented for channels with various breadth distributions. The sides of the channel are taken to be parallel on the intervals $[x_e, 0]$ and $[10, x_o]$, where $x_e = -l$ and $x_o = 10 + l$ for different values of l. The breadth varies only on

the interval [0, 10]; in this way any inconsistencies in the definition of the boundary function C can be studied. The breadth distributions used are

$$B_4(x) = \begin{cases} 6+4\left(1-\frac{x}{5}\right)^2 & x \in [0,10] \\ 10 & x \in [-l,0] \cup [10,10+l], \end{cases}$$

$$B_5(x) = \begin{cases} 10 & x \in [-l,0] \\ 6+4\left(1-\frac{x}{5}\right)^2 & x \in [0,8] \\ 6+4\left(\frac{3}{5}\right)^2 & x \in [8,10+l], \end{cases}$$

$$B_6(x) = \begin{cases} 6+4\left(1-\frac{x}{3}\right)^2 & x \in [0,3] \\ 6+4\left(\frac{3}{7}-\frac{x}{7}\right)^2 & x \in [3,10] \\ 10 & x \in [-l,0] \cup [10,10+l]. \end{cases}$$

The initial approximation, ϕ^0 , to ϕ is given by

$$\phi_i^0 = \left(\frac{x_i - x_e}{x_2 - x_1}\right) v^0 \quad i = 1, \dots, p,$$
(4.31)

where v^0 is assigned a value which determines whether the subcritical or supercritical approximation is calculated. In theory, if $v^0 < c_* \frac{x_o - x_e}{n-1}$ the algorithm generates the subcritical solution and if $v^0 > c_* \frac{x_o - x_e}{n-1}$ the supercritical solution is found.

The energy E is taken to be 50. Two types of boundary conditions are employed. The first is that C(y) = -K, where K is a constant, on Σ_e and $C(y) = \frac{KB_e}{B_o}$ on Σ_o which is consistent with conservation of mass. The second boundary condition is given by $C(y) = K_1 + K_2 y$ on Σ_e and $C(y) = -(K_1 + K_2 y)$ on Σ_o where K_1 and K_2 are given constants and $B_e = B_o$.

Results are given for the first type of boundary condition with K=10.

Consider the breadth distribution $B_4(x)$ with l=1, n=5 and m=3. For this domain Newton's method, with a tolerance in (4.10) of 10^{-3} , converges to the subcritical approximation in 4 iterations requiring respectively 5, 7, 7 and 8 conjugate gradient iterations with a tolerance of 10^{-1} . On a refined grid, with l=1, n=7 and m=5, and using the same tolerances, Newton's method converges to the subcritical approximation in 5 iterations requiring 12, 13, 15, 16 and 5 conjugate gradient iterations. In both cases ϕ^0 is given by (4.31) with $v^0=0$. Both of the approximations exhibit the property of the exact subcritical solution that the speed increases as the channel breadth decreases. They also approximately satisfy the boundary conditions of zero flow across the channel sides and the axis of symmetry y=0. The change in the approximate speed with breadth is represented better on the refined grid, in particular the maximum speed has increased and the minimum decreased. Increasing the resolution of a more refined grid has less effect on the velocity approximation.

Two-dimensional approximations to supercritical flows were not found accurately by this method. The best results were generated by using the supercritical

one-dimensional approximation to ϕ , calculated in Section 4.1.2, as the initial approximation ϕ^0 , that is,

$$\phi_{i+(j-1)n}^0 = \hat{\phi}_i \quad i = 1, \dots, n, \ j = 1, \dots, m,$$

where $\hat{\boldsymbol{\phi}}=(\hat{\phi}_1,\ldots,\hat{\phi}_n)^T$ is the one-dimensional solution vector. Then, using $B_4(x)$ with $l=5,\ n=5$ and m=3, the ratio $\frac{\max_i |\delta \phi_i^k|}{\max_i |\phi_i^k|}$ reached a minimum of 2.35×10^{-2} for 4 Newton iterations but increased as the iterations continued. The approximate solution at k=4 is shown in Figure 9. This is the piecewise constant velocity approximation calculated from $\mathbf{v}^h=\nabla\phi^h$ on each element, the length of the arrow in each element being directly proportional to the magnitude of \mathbf{v}^h . The failure of the method to converge completely in this case might be the result of the occurrence of a hydraulic jump in the supercritical flow for the shapes of channel considered. The approximation does exhibit certain properties of the exact solution in that the magnitude of the supercritical velocity decreases as the channel breadth decreases and the flow directions appear to be approximately consistent with the boundary conditions of zero flow across the channel sides and the line of symmetry y=0.

Figures 10 and 11 show approximations \mathbf{v}^h to the velocity for subcritical flows. The breadth variation in each case is $B_4(x)$ and several values of l are considered.

Figure 10 is the approximation for l=1, n=9 and m=7. The increase in the magnitude of the velocity as the breadth decreases can be clearly seen and this agrees with the behaviour of exact subcritical solutions. Notice also that the speed is greater close to the x-axis than it is near the channel sides.

Figure 11 shows the consequences of increasing the lengths of the sections of the channel where the sides are parallel. In Figure 11a l=15 and in Figure 11b l=5. It can be seen that increasing l from 5 to 15 has very little affect on the approximation in the region between the lines x=-5 and x=15. Also notice that the velocity in the domain $\{(x,y):x\in[-15,-5],y\in[0,B(x)]\}$ is virtually constant and parallel to the channel sides.

This justifies the use of the boundary conditions C(y) = -K on Σ_e and $C(y) = \frac{KB_e}{B_o}$ on Σ_o for $l > \sim 5$ which should ideally be applied at the ends of an infinitely long channel since they assume that the flow is uniform across the inlet and outlet cross sections.

Thus, the algorithm given in this section can be used to generate a twodimensional piecewise constant approximation to the subcritical velocity in channels of various breadth distributions.

The methods of this section are all concerned with approximating continuous solutions of the shallow water equations of motion. In Section 5 approximations to discontinuous solutions are considered.

5 Solutions on Variable Grids

In order to be able to approximate discontinuous shallow water flows and to improve approximations to continuous flows, methods of generating grid dependent solutions are now considered.

First, the constrained 'r' principle (2.19) is used to generate a piecewise linear approximation to a discontinuous depth variation on a grid with just one adjustable node. This node is placed at the discontinuity by applying the jump conditions of Section 3. The method is modified slightly to generate approximations to continuous depth variations on variable grids. This idea is extended further to give a second algorithm for approximating discontinuous solutions. Finally, the constrained 'p' principle (2.18) is used to generate piecewise linear approximations to the velocity potential on a solution dependent grid generated directly from the variational principle.

5.1 The Constrained 'r' Principle

5.1.1 Grid with One Moving Node

Consider the constrained one-dimensional 'r' principle (2.19). Let the domain of integration, $[x_e, x_o]$, be split into n-1 adjacent intervals by the points x_i (i = 1, ..., n) given by (4.10). In order to approximate discontinuous flows one of these grid points must be chosen to be the initial approximation to the position of the discontinuity. This requires deducing which of the nodes is nearest to the actual position of the hydraulic jump. Let N = n-1 be the initial guess for the number of this node in the grid given by (4.10).

The basis of the method to approximate discontinuous flows is to generate approximate solutions in front of the jump and behind the jump and to couple the two approximations by means of a discontinuity at the position of the jump.

The energy E of the flow in front of the jump is given by the specified value E^e . Let the approximation to the depth in this region, $[x_1, x_N]$, be

$$d^{e}(x) = \sum_{i=1}^{N} d_{i}^{e} \alpha_{i}^{e}(x),$$

where

$$\alpha_{1}^{e}(x) = \begin{cases} \frac{x_{2}-x}{x_{2}-x_{1}} & x \in [x_{1}, x_{2}] \\ 0 & x \notin [x_{1}, x_{2}] \end{cases},$$

$$\alpha_{i}^{e}(x) = \begin{cases} \frac{x-x_{i-1}}{x_{i}-x_{i-1}} & x \in [x_{i-1}, x_{i}] \\ \frac{x_{i+1}-x_{i}}{x_{i+1}-x_{i}} & x \in [x_{i}, x_{i+1}] \\ 0 & x \notin [x_{i-1}, x_{i+1}] \end{cases} i = 2, \dots, N-1,$$

$$\alpha_N^e(x) = \begin{cases} \frac{x - x_{N-1}}{x_N - x_{N-1}} & x \in [x_{N-1}, x_N] \\ 0 & x \notin [x_{N-1}, x_N] \end{cases}.$$

The energy E of the flow behind the jump is E° , which is calculated from the specified outlet depth using conservation of mass and the definitions of mass flow and energy E (2.1) and (2.2). Let the approximation to the depth in the region $[x_N, x_n]$ be given by

$$d^{o}(x) = \sum_{i=N}^{n} d_{i}^{o} \alpha_{i}^{o}(x),$$

where

$$\alpha_{N}^{o}(x) = \begin{cases} \frac{x_{N+1} - x}{x_{N+1} - x_{N}} & x \in [x_{N}, x_{N+1}] \\ 0 & x \notin [x_{N}, x_{N+1}] \end{cases},$$

$$\alpha_{i}^{o}(x) = \begin{cases} \frac{x - x_{i-1}}{x_{i} - x_{i-1}} & x \in [x_{i-1}, x_{i}] \\ \frac{x_{i+1} - x}{x_{i+1} - x_{i}} & x \in [x_{i}, x_{i+1}] \\ 0 & x \notin [x_{i-1}, x_{i+1}] \end{cases} \quad i = N+1, \dots, n-1,$$

$$\alpha_{n}^{o}(x) = \begin{cases} \frac{x - x_{n-1}}{x_{n} - x_{n-1}} & x \in [x_{n-1}, x_{n}] \\ 0 & x \notin [x_{n-1}, x_{n}] \end{cases}.$$

The discontinuous approximation is given by the values of $\mathbf{d}^e = (d_1^e, \dots, d_N^e)^T$, $\mathbf{d}^o = (d_N^o, \dots, d_n^o)^T$ and x_N such that

$$L\left(\mathbf{d}^{e}, \mathbf{d}^{o}, x_{N}\right) = \int_{x_{1}}^{x_{N}} B\left(r\left(Q, d^{e}\right) + E^{e} d^{e}\right) dx + \int_{x_{N}}^{x_{n}} B\left(r\left(Q, d^{o}\right) + E^{o} d^{o}\right) dx \quad (5.1)$$

is stationary with respect to variations in \mathbf{d}^e , \mathbf{d}^o and x_N . The algorithm which generates the approximation is in two parts.

First, with the grid points fixed, seek the supercritical solution \mathbf{d}^e such that the functional L in (5.1) is stationary with respect to variations in \mathbf{d}^e . This is done using Newton's method as in Section 4.1.1. Also, seek the subcritical solution \mathbf{d}^o such that L is stationary with respect to variations in \mathbf{d}^o by the same method.

The approximation, x_N , to the position of the jump is improved by employing the jump condition. If x_s is the exact position of the discontinuity and d is the exact solution then, from (3.9), the jump condition is

$$(r(Q,d) + E^e d)|_{x_{a+}} - (r(Q,d) + E^o d)|_{x_{a-}} = 0.$$

If

$$\left| (r(Q, d^e) + E^e d^e) \right|_{x_N} - (r(Q, d^o) + E^o d^o) \right|_{x_N} \right| < \text{tolerance},$$
 (5.2)

for some specified tolerance, then the approximate solution has been found and x_N is the approximate position of the hydraulic jump. If (5.2) is not satisfied then a new approximation to the jump position is found using the jump condition as follows.

The equation

$$r(Q_s, d_N^e) + E^e d_N^e - r(Q_s, d_N^o) - E^o d_N^o = 0$$
(5.3)

is solved to give the value, Q_s , of the mass flow which would occur at the jump if d_N^e and d_N^o were the actual depths of the flow before and after the jump. The 'r' principle (2.19), and therefore (5.1), is constrained to satisfy conservation of mass, that is,

$$Q(x)B(x) = CB_e \quad x \in [x_e, x_o]. \tag{5.4}$$

Since the breadth distribution is to be specified, (5.4) can be used to find the point x_s^N in the channel where the mass flow is of magnitude Q_s . Using the known breadth variation, B(x), on the outlet section of the channel the value of x_s^N is found by bisection from

$$B\left(x_s^N\right) = \frac{CB_e}{Q_s}. (5.5)$$

It is conjectured that the point x_s^N is closer to the actual jump position than the point x_N .

The algorithm for positioning a node at the jump is in two parts. Firstly, beginning with N=n-1 the corresponding value of x_s^{n-1} is found. Then, stepping backwards along the channel to the n-2 th node, the value of x_s^{n-2} is found. If $(x_{n-1}-x_s^{n-1})(x_{n-2}-x_s^{n-2})<0$ then x_s lies between x_{n-2} and x_{n-1} . Otherwise the process is repeated until the node j is found such that $(x_j-x_s^j)(x_{j-1}-x_s^{j-1})<0$. Then, if $|x_j-x_s^j|<|x_{j-1}-x_s^{j-1}|$, the number, N, of the node to be moved to the jump position is j; otherwise N=j-1.

Once the number of the node to be moved to the jump position has been established (5.3) is used in an iteration process to position the node at the jump. The node x_N is moved to the position x_s^N which is calculated from (5.3) and (5.5). The finite element approximation to d is re-calculated on the modified grid and if (5.2) is still not satisfied (5.3) is solved for Q_s then (5.5) yields a new x_s^N . The node x_N is moved to x_s^N and the process is repeated until (5.2) is satisfied. The approximate solution has then been found and x_N is an approximation to the jump position.

The algorithm is applied to a grid with $x_e = 0$, $x_o = 10$ and n = 21. The breadth distributions considered here are

$$B_7(x) = 6 + 4\left(1 - \frac{x}{5}\right)^k \ x \in [x_e, x_o], \quad k = 2, 4.$$

The energy E is taken to be 50 and the mass flow at inlet C is assigned the value which causes the flow to become critical at the channel throat, that is, C = 11.5.

Under these conditions, for a tolerance on the Newton iteration of 10^{-3} and on the jump condition (5.2) of 10^{-3} , the method converges to a discontinuous

approximation, with outlet depth specified to be 4.6, in 4 iterations on the position of the discontinuity once the node to be placed at the discontinuity has been found. These iterations require 11, 8, 6 and 6 Newton iterations. The initial values of the approximation at the nodes of the original, regular grid are $d_i^e = 1$ (i = 1, ..., N) and $d_i^o = 4.6$ (i = N, ..., n). Once the number of the node to approximate the jump position has been deduced, subsequent approximations to the finite element solution use the approximation on the previous grid as the first guess in Newton's method to find the approximation on the new grid.

Figure 12 gives a result for $B_7(x)$ (k=4). Figure 12a is an approximation to discontinuous flow caused by specifying the outlet depth to be 4.68; the flow is supercritical before the jump and subcritical afterwards. The number of the node which has been moved to the jump position is 15. Figure 12b is the linear interpolation of the breadth function at the grid points.

The algorithm given in this section is a method for generating an approximation to a discontinuous flow in a channel, given the energy and mass flow at inlet, the breadth distribution and the depth at outlet. It uses a grid where all of the nodes except one are fixed. The algorithm causes the one movable node to be located at the position of the hydraulic jump.

In Sections 5.1.2 and 5.1.3 this method is extended and applied to a grid where all the internal nodes are allowed to vary.

5.1.2 Grid Dependent Solutions

In this section the constrained 'r' principle (2.19) is used to calculate a piecewise linear approximation to the depth on a solution dependent grid where all the internal grid points are allowed to move.

The domain of integration $[x_e, x_o]$ is divided into n-1 adjacent intervals by the points x_i (i = 1, ..., n) given by (4.10). The method is to generate finite element approximations to the depth on each interval $[x_i, x_{i+1}]$ (i = 1, ..., n-1) and use the jump condition at each internal node to reposition the node. Instead of just two finite element approximations coupled at a point, as in Section 5.1.1, there are now n-1 solutions coupled at the n-2 internal nodes.

Let $d_i^h(x)$ be the finite element approximation to d in the i th element, $[x_i, x_{i+1}]$, given by

$$d_i^h(x) = d_i^L \alpha_i^L(x) + d_i^R \alpha_i^R(x) \quad i = 1, \dots, n-1,$$
 (5.6)

where

$$\alpha_i^L(x) = \begin{cases}
\frac{x_{i+1} - x}{x_{i+1} - x_i} & x \in [x_i, x_{i+1}] \\
0 & x \notin [x_i, x_{i+1}]
\end{cases} i = 1, \dots, n-1,$$

$$\alpha_i^R(x) = \begin{cases}
\frac{x - x_i}{x_{i+1} - x_i} & x \in [x_i, x_{i+1}] \\
0 & x \notin [x_i, x_{i+1}]
\end{cases} i = 1, \dots, n-1.$$
(5.7)

The finite element solution on each element is given by the values of $\mathbf{d}_i = (d_i^L, d_i^R)^T$ such that

$$L\left(\mathbf{d}_{1},\ldots,\mathbf{d}_{n-1}\right) = \int_{x_{1}}^{x_{n}} B\left(r\left(Q,d^{h}\right) + Ed^{h}\right) dx \tag{5.8}$$

is stationary with respect to variations in \mathbf{d}_i (i = 1, ..., n - 1). The solutions are found using Newton's method, as previously, except that there are now n - 1 problems, each with 2 unknowns.

Once $\mathbf{d}_1, \ldots, \mathbf{d}_{n-1}$ have been calculated, the positions of the internal nodes are allowed to vary using the jump conditions. If

$$\left| \left(r \left(Q, d_i^h \right) + E d_i^h \right) \right|_{x_i} - \left(r \left(Q, d_{i-1}^h \right) + E d_{i-1}^h \right) \right|_{x_i} \right| < \text{tolerance}$$
 (5.9)

for a specified tolerance and for all i = 2, ..., n - 1, the required approximation has been found. If (5.9) is not satisfied for any value of i = 2, ..., n - 1, the new position of the grid point is found by solving

$$r(Q_s, d_i^L) + Ed_i^L - r(Q_s, d_{i-1}^R) - Ed_{i-1}^R = 0$$

for Q_s . The new position for x_i is calculated from Q_s using the conservation of mass equation and bisection. The finite element solutions are found for the new grid and the procedure is repeated until (5.9) is satisfied.

The algorithm is applied to a channel where the breadth distribution is given by

$$B_8(x) = 10 + 2 \tanh\left(\frac{x-8}{0.43}\right) - 2 \tanh\left(\frac{x-2}{0.43}\right) \ x \in [x_e, x_o], \tag{5.10}$$

where $x_e = 0$, $x_o = 10$ and n = 21. The energy E is taken to be 50 and the mass flow at inlet, C, is assigned the value which causes the flow to be critical at the channel throat, that is C = 11.5.

Figure 13a shows the subcritical approximation to the depth under these conditions. A piecewise linear interpolation of the breadth function is given in Figure 13b. The dots in Figure 13a are the final positions of the grid points. There is a slight movement of the nodes to regions where the breadth function has highest curvature. These correspond to regions where the depth function also has highest curvature and so improve the piecewise linear approximation from the case of a fixed, regular grid. Notice that the jump in the value of the depth approximation at each node is small, that is, the discontinuous piecewise linear depth approximation is nearly continuous.

5.1.3 Discontinuous Grid Dependent Approximations

The methods of Sections 5.1.1 and 5.1.2 are combined to create an algorithm for generating approximations to discontinuous depth solutions on solution dependent grids using the constrained 'r' principle (2.19).

The domain $[x_e, x_o]$ is divided into the n-1 intervals $[x_i, x_{i+1}]$ (i = 1, ..., n-1) by the points x_i (i = 1, ..., n) given by (4.10). Let $d_i^h(x)$ be the finite element approximation to d in the i th element $[x_i, x_{i+1}]$ where $d_i^h(x)$ is defined by (5.6) and the basis functions are given by (5.7).

The solutions $\mathbf{d}_i = (d_i^L, d_i^R)^T$ are sought such that (5.8) is stationary with respect to \mathbf{d}_i for i = 1, ..., n - 1. The energy E in the integrand of (5.8) is assigned a value depending on whether the i th interval is in front of or behind the node which is chosen to be the initial approximation to the position of the hydraulic jump. Let the number of this chosen node be N then

$$E = E^e \quad \text{if} \quad i+1 \le N$$
and
$$E = E^o \quad \text{if} \quad i \ge N,$$

where E^e is the value of E at inlet and E^o is the value of E at outlet which is calculated from the specified value of the outlet depth.

The solutions \mathbf{d}_i (i = 1, ..., n - 1) are found using Newton's method, as previously.

Once the \mathbf{d}_i $(i = 1, \dots, n-1)$ have been calculated on the initial grid the jump condition is applied at each internal node. If

$$\left| \left(r \left(Q, d_i^L \right) + E_1 d_i^L \right) \right|_{x_i} - \left(r \left(Q, d_{i-1}^R \right) + E_2 d_{i-1}^R \right) \right|_{x_i} < \text{tolerance}, \tag{5.11}$$

where

$$E_1 = E_2 = E^e$$
 if $i < N$,
 $E_1 = E^o$, $E_2 = E^e$ if $i = N$,
 $E_1 = E_2 = E^o$ if $i > N$,

for all i = 1, ..., n-1 and given a specified tolerance, the required approximation has been found. If (5.11) is not satisfied for a certain value of i then the new position of the corresponding grid point, x_i , is found by solving

$$r(Q_i, d_i^L) + E_1 d_i^L - r(Q_i, d_{i-1}^R) - E_2 d_{i-1}^R = 0$$
(5.12)

for Q_i . The new value for x_i is found from Q_i using the conservation of mass law and bisection.

The grid point closest to the jump position is found in the same way as in the method of Section 5.1.1. The approximation, x_N , to the jump position is initially taken to be x_{n-1} ; equation (5.12) then yields a better approximation x_s^{n-1} to the jump position. The process is repeated next using x_{n-2} as the approximation to the jump position and then continuing back along the channel using each grid point in turn until $(x_{j-1} - x_s^{j-1})(x_j - x_s^j) < 0$ for some j. Then, if $|x_j - x_s^j| < |x_{j-1} - x_s^{j-1}|$, N = j is the number of the node which will be moved to the jump position; otherwise N = j - 1.

With N fixed the n-1 finite dimensional approximations (5.6) are calculated on the new grid using the solution on the previous grid as the initial guess in Newton's method. If (5.11) is not satisfied for some i in the range $1, \ldots, n$ the grid points are repositioned using (5.12). The process is repeated until (5.11) is satisfied for all i in the range $1, \ldots, n$. An approximation to a discontinuous shallow water flow has then been found.

The algorithm is applied on a domain where $x_e = 0$, $x_o = 10$ and the breadth distribution is given by

$$B_9(x) = 6 + 4\left(1 - \frac{x}{5}\right)^k \quad x \in [x_e, x_o] \quad k = 2, 4.$$

The number of grid points n = 21. The energy E is taken to be 50 and the mass flow at inlet C is given the value which causes the flow to be critical at the channel throat, that is C = 11.5.

Figure 14 gives solutions for the breadth distribution $B_9(x)$ (k=2). Figure 14a shows the depth approximation for an outlet depth of 4.6. The number of the node which is placed at the jump position is 15. Figure 14b is the piecewise linear interpolation to the breadth function using the 21 grid points. The position of the 15th node has moved to be at the jump position from its initial location. The other nodes have hardly moved, the curvature of the breadth function not being as large as, for example, that of the breadth function given by (5.10). Given a tolerance in (5.11) of 0.5 the method converges in 4 iterations on nodal positions. Figure 14c is the corresponding depth approximation for an outlet depth of 4.0 which, for the same tolerance, converges in 5 iterations.

The methods of Sections 5.1.1, 5.1.2 and 5.1.3 yield piecewise linear approximations to continuous and discontinuous depth functions. They use the jump condition derived in Section 3 to create solution dependent grids. An alternative method is now described using the constrained 'p' principle (2.18) to generate a piecewise linear approximation to the velocity potential on a variable grid.

5.2 The Constrained 'p' Principle

Consider the one-dimensional constrained 'p' principle (2.18).

Let the domain of integration $[x_e, x_o]$ be divided into n-1 intervals $[x_i, x_{i+1}]$ (i = 1, ..., n-1) by the points x_i (i = 1, ..., n) given by (4.10). Let

$$\phi^{h}(x, \mathbf{x}) = \sum_{i=1}^{n} \phi_{i} \alpha_{i}(x, x_{i-1}, x_{i}, x_{i+1})$$

be the finite element approximation to the velocity potential ϕ . The basis func-

tions α_i (i = 1, ..., n) are the piecewise linear basis functions given by

$$\alpha_{1}(x, x_{1}, x_{2}) = \begin{cases} \frac{x_{2} - x}{x_{2} - x_{1}} & x \in [x_{1}, x_{2}] \\ 0 & x \notin [x_{1}, x_{2}] \end{cases},$$

$$\alpha_{i}(x, x_{i-1}, x_{i}, x_{i+1}) = \begin{cases} \frac{x - x_{i-1}}{x_{i} - x_{i-1}} & x \in [x_{i-1}, x_{i}] \\ \frac{x_{i+1} - x}{x_{i+1} - x_{i}} & x \in [x_{i}, x_{i+1}] \\ 0 & x \notin [x_{i-1}, x_{i+1}] \end{cases} \qquad i = 2, \dots, n-1,$$

$$\alpha_{n}(x, x_{n-1}, x_{n}) = \begin{cases} \frac{x - x_{n-1}}{x_{n} - x_{n-1}} & x \in [x_{n-1}, x_{n}] \\ 0 & x \notin [x_{n-1}, x_{n}] \end{cases},$$

the ϕ_i (i = 1, ..., n) are the values of the approximation at the x_i and $\mathbf{x} = (x_1, ..., x_n)^T$ is the vector of nodes of the grid. The discrete version of the functional in (2.19) is given by

$$L\left(\boldsymbol{\phi},\mathbf{x}\right) = \left(\int_{x_1}^{x_2} + \dots + \int_{x_{n-1}}^{x_n}\right) Bp\left(\phi^{h'}, E\right) dx + CB_e\left(\phi^{h}\left(x_n, \mathbf{x}\right) - \phi^{h}\left(x_1, \mathbf{x}\right)\right)$$

where $\phi = (\phi_1, \dots, \phi_n)^T$ and ${\phi^h}' \equiv \frac{\partial \phi^h}{\partial x}$. The finite element solution for the velocity potential is found by solving the set of equations

$$F_{i}(\boldsymbol{\phi}, \mathbf{x}) = \frac{\partial L}{\partial \phi_{i}} = \left(\int_{x_{1}}^{x_{2}} + \dots + \int_{x_{n-1}}^{x_{n}} \right) B p_{\phi^{h'}} \alpha_{i}' dx + C B_{e} \left[\alpha_{i} \right]_{x_{1}}^{x_{n}} = 0 \quad i = 1, \dots, n$$
(5.13)

for ϕ . This is done by Newton's method, as previously.

New positions for the grid nodes are found by solving

$$G_{i}(\boldsymbol{\phi}, \mathbf{x}) = \frac{\partial L}{\partial x_{i}} = [-Bp]_{x_{i}} + \left(\int_{x_{1}}^{x_{2}} + \dots + \int_{x_{n-1}}^{x_{n}}\right) Bp_{\phi^{h'}} \frac{\partial \phi^{h'}}{\partial x_{i}} dx$$
$$+ CB_{e} \left[\frac{\partial \phi^{h}}{\partial x_{i}}\right]_{x_{1}}^{x_{n}} = 0 \quad i = 2, \dots, n-1$$
 (5.14)

for x_i (i = 2, ..., n - 1) by Newton's method.

The process of solving alternately (5.13) and (5.14) is repeated until either

$$\max_{i} \left(\left| \frac{\partial L}{\partial \phi_{i}} \right|, \left| \frac{\partial L}{\partial x_{i}} \right| \right) < \text{tolerance}$$

or until successive values of

$$\max \left(\max_{i} \left| \frac{\partial L}{\partial \phi_{i}} \right|, \max_{i} \left| \frac{\partial L}{\partial x_{i}} \right| \right) \tag{5.15}$$

for the solutions change by less than some percentage.

Consider the domain [-5, 15]. Several breadth distributions are studied. These are

$$B_{10}(x) = \begin{cases} 6+4\left(1-\frac{x}{5}\right)^k & x \in [0,10] \\ 10 & x \in [-5,0] \cup [10,15] \end{cases} \quad k = 2, 4, 6, 12,$$

$$B_{11}(x) = \begin{cases} 8 + 2\cos\left(\frac{\pi x}{5}\right) & x \in [0, 10] \\ 10 & x \in [-5, 0] \cup [10, 15] \end{cases},$$

$$B_{12}(x) = \begin{cases} 10 + 2\tanh 2(x - 8) + 2\tanh 2(2 - x) & x \in [0, 10] \\ 10 & x \in [-5, 0] \cup [10, 15] \end{cases}.$$

The energy E is assigned the value 50 and the mass flow at inlet C = 11.5. Let the criterion for convergence using (5.15) be that the value of (5.15) changes by less than 5%.

Consider a domain where the breadth is given by B_{11} . Let the number of grid points n = 9. Then the method converges to the subcritical approximation in 11 iterations on the nodal positions, to the supercritical approximation in 3 iterations and to a transitional approximation in 17 iterations.

The associated piecewise constant velocity approximations, calculated using $v^h = \phi^{h'}$, are shown in Figure 15. Figure 15a shows the supercritical approximation. The grid points have not moved from their original positions given by (4.10). The subcritical approximation is given in Figure 15b. The grid points have moved towards the midpoint of the channel, that is, towards the region where the curvature of the breadth is largest. Figure 15c shows an approximation to transitional flow where the flow is supercritical at inlet, becomes critical at the channel throat and then subcritical in the outlet section. Figure 15d shows the breadth variation.

Figure 16 gives corresponding results for a grid with 41 nodes. There is a slight node movement in the subcritical case (Figure 16b) and none at all in the supercritical case (Figure 16a).

6 Acknowledgements

I thank Dr. M. J. Baines and Dr. D. Porter for their help with this work. I acknowledge receipt of an SERC research studentship.

7 References

- [1] S. L. Wakelin. Variational Principles for Free Surface Flows. Numerical Analysis Report 4/92, University of Reading.
- [2] J. C. Luke. A Variational Principle for a Fluid with a Free Surface. J. Fluid Mech. 27 (1967) 395–397.
- [3] J. J. Stoker. Water Waves. Interscience, 1957.

- [4] R. Courant and D. Hilbert. Methods of Mathematical Physics Vol. 1. Interscience, 1953.
- [5] G. H. Golub and C. F. Van Loan. Matrix Computations. The John Hopkins University Press, Baltimore, Maryland, U.S.A., 1989 (2nd Ed.).
- [6] A. J. Wathen. Realistic Eigenvalue Bounds for the Galerkin Mass Matrix. I.M.A. J. Numer. Anal. 7 (1987) 449–457.

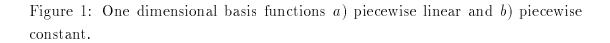


Figure 2: a) Depth approximations on a fixed grid and b) $B_1(x)$ (k = 8).

Figure 3: a) Depth approximations on a fixed grid and b) $B_3(x) \nu = 7.5$, $\sigma = 1.5$.

Figure 4: a) $B_1(x)$ (k = 2), b) supercritical velocity and c) velocity potential approximations on a fixed grid.

Figure 5: a)Mass flow, b) velocity potential , c) depth and d) velocity approximations on a fixed grid — supercritical case.

Figure 6: a)Mass flow, b) velocity potential , c) depth and d) velocity approximations on a fixed grid — subcritical case.

Figure 7: Example of a two-dimensional grid for $B_4(x)$ (k=2) with n=9 and m=7.

Figure 8: Two-dimensional basis function.

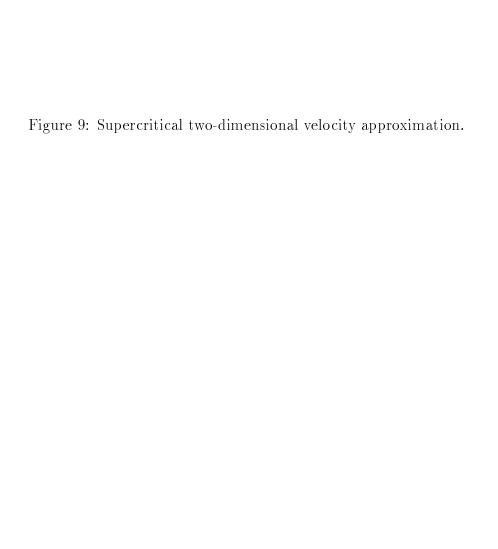


Figure 10: Subcritical two-dimensional velocity approximation.

Figure 11: Subcritical two-dimensional velocity approximations — a) l=15 and b) l=5.

Figure 12: a) Depth approximation on grid with one moving node $(d_o = 4.68)$ and b) $B_7(x)$ (k = 2).

Figure 13: a) Subcritical depth approximation on an adaptive grid and b) $B_8(x)$.

Figure 14: a) Depth approximation on adaptive grid $(d_o = 4.6)$, b) $B_9(x)$ (k = 2) and c) depth approximation $(d_o = 4.0)$.

Figure 15: Adaptive grid with n=9 a) supercritical velocity approximation, b) subcritical velocity approximation, c) transitional velocity approximation and d) $B_{11}(x)$.

Figure 16: Adaptive grid with n=41 a) supercritical velocity approximation, b) subcritical velocity approximation, c) transitional velocity approximation and d) $B_{11}(x)$.